Applied Catalysis B: Environmental 237 (2018) 149–157

Contents lists available at ScienceDirect

Applied Catalysis B: Environmental

journal homepage: www.elsevier.com/locate/apcatb

Acrolein production from methanol and ethanol mixtures over La- and Ce-doped FeMo catalysts

Anita Borowiec[a], Aleksandra Lilić[b], Jean-Charles Morin[a], Jean-François Devaux[c], Jean-Luc Dubois[d], Simona Bennici[e], Aline Auroux[b], Mickaël Capron[a,*], Franck Dumeignil[a]

[a] Univ. Lille, CNRS, Centrale Lille, ENSCL, Univ. Artois, UMR 8181 - UCCS - Unité de Catalyse et Chimie du Solide, F-59000, Lille, France
[b] IRCELYON, UMR 5256 CNRS- Université Lyon 1, 2 avenue Albert Einstein, 69626, Villeurbanne cedex, France
[c] Arkema France, rue Henri Moissan, 69491, Pierre Bénite cedex, France
[d] Arkema France, 420 Rue d'Estienne d'Orves, 92705, Colombes, France
[e] Institut de Science des Matériaux de Mulhouse (IS2M), UMR 7361 CNRS-UHA, Mulhouse Cedex, France

ARTICLE INFO

Keywords:
Acrolein
Alcohols coupling
Oxidation
Iron-molybdate
Heterogeneous catalysis

ABSTRACT

The acrolein production from methanol and ethanol mixtures over iron-molybdate-based catalysts was studied. The reaction to acrolein can be described by two successive steps: the first consists on the oxidation of both alcohols into their corresponding aldehydes and the second step is the subsequent aldol condensation of the as-formed aldehydes. The iron-molybdate catalysts were modified by doping with La and Ce (1%mol) in order to improve the aldol condensation step of the process. Series of catalysts were thus synthesized with different Mo/Fe ratios (i.e., 1.5, 2.0 and 2.5) and calcined at three different temperatures (i.e, 350 °C, 400 °C and 450 °C). The best catalytic performance was observed for FeMoCe2.0 (400 °C) for which the acrolein yield reached 42% (T = 320 °C, MetOH/EtOH = 1, GHSV = 3900 h^{-1}). Furthermore, all the samples were characterised by TGA-DSC, HT-XRD, XPS, BET, LEIS, XRF, CO_2-TPD, Pyridine (FTIR) and NH_3 (calorimetry) adsorption. The increase in acrolein yield observed upon La and Ce doping was attributed to acid/base properties modification.

1. Introduction

Acrolein (propenaldehyde) is the simplest unsaturated aldehyde, which finds numerous applications in the chemical industry. Its most important use is the production of acrylic acid applied in the manufacturing of coating resins, polyacrylic acid (rheology modifiers), superabsorbents, detergents and others. The second main acrolein application is the production of methionine, which is an essential amino acid used for cattle feed and battery farming. Until now, the main method of acrolein production is propylene oxidation. However, the increasing demand as well as environmental requirements generated active research of alternative processes [1,2,3,4,5,6,7,8]. Unfortunately, due to the feedstock unstable prices and scaling-up issues, these methods cannot actually be used at the large scale. Recently, a new method of acrolein production was shown, [9,10,11,12] based on methanol and ethanol as raw materials. The mentioned feedstock can be obtained from biomass at competitive prices. This reaction can be schematically described as two concomitant steps, namely alcohol oxidation (Eq. (1)) and the as-formed aldehyde aldol condensation to acrolein (Eq. (2)):

$$CH_3OH + C_2H_5OH + O_2 \rightarrow HCHO + CH_3CHO + 2\,H_2O \quad (1)$$

$$HCHO + CH_3CHO \rightarrow CH_2CHCHO + H_2O \quad (2)$$

Note that the transformation of the alcohols into aldehydes (Eq. (1)) can also result from a dehydrogenation reaction, but for valorization of acrolein, very low propanaldehyde contents are necessary. This reaction has been achieved in the gas phase with the use of iron molybdate mixed oxides in one reactor, a catalytic system extensively described elsewhere [13,14] and industrially used to perform the methanol oxidation to formaldehyde [15]. This heterogeneous catalyst is composed of two major phases [2,16,17,18]: MoO_3 (#PDF 01-089-5108) and $Fe_2(MoO_4)_3$ (#PDF 00-031-0642), of which the relative proportion is closely related to the Mo/Fe ratio used during the preparation of the solid. This catalyst exhibits both an acidic and a redox behavior, the latter which is necessary for the considered reaction; while the former was evidenced in methanol rich oxidation condition by the formation of dimethoxymethane [19,20]. It has to be noted that the aldol condensation reaction can proceed as well over acid or basic sites. The presence of the acid sites over the FeMo formulation was previously attributed mainly to the creation of anionic vacancies acting as Lewis acid sites produced by dehydroxylation of the catalyst surface (upon reduction in the reactants atmosphere), while the redox properties are

* Corresponding author.
E-mail address: mickael.capron@univ-lille1.fr (M. Capron).

https://doi.org/10.1016/j.apcatb.2018.05.076
Received 13 February 2018; Received in revised form 19 May 2018; Accepted 27 May 2018
Available online 28 May 2018
0926-3373/

provided by the Fe active sites.

The bifunctional behavior of such a catalytic system, due to the synergetic effect between an adequate number of Mo sites and Fe sites, is crucial for the efficient conversion of methanol and ethanol mixtures to acrolein.

The aim of the present study was to improve the FeMo formulation to increase the acrolein yield by doping with La and Ce in order to tune the acid/base properties of the catalysts. The materials were prepared, characterized and their catalytic activity was measured in a fixed bed reactor in the gas phase.

2. Experimental

2.1. Materials

Ammonium molybdate tetrahydrate $(NH_4)_6Mo_7O_{24}{\cdot}4H_2O$ (AHM, Fluka, 99%), iron (III) chloride hexahydrate $FeCl_3{\cdot}6H_2O$ (Sigma-Aldrich, 97%), lanthanum (III) nitrate hexahydrate $La(NO_3)_3{\cdot}6H_2O$ (Aldrich, 99.99%), cerium (III) nitrate hexahydrate $Ce(NO_3)_3{\cdot}6H_2O$ (Aldrich, 99.99%), stearic acid $C_{17}H_{35}COOH$ (Sigma-Aldrich, 98.5%), sodium chloride NaCl (Fluka, 99%), silver nitrate $AgNO_3$ (Aldrich, 99.99%), ethanol C_2H_5OH (Sigma-Aldrich, 99.8%), methanol CH_3OH (Sigma-Aldrich, 99.8%), helium (Air Liquide, alphagaz 99.9%) and oxygen (Air Liquide, 99.9%) were used as such without a further purification step.

2.2. Doped iron molybdate catalysts synthesis

The iron molybdate catalysts were synthetized using a coprecipitation method described by Pernicone et al. [17,21,22]. In the case of the reference FeMo catalyst, aqueous solutions of AHM and iron (III) chloride hexahydrate were prepared based on a Mo/Fe ratio equal to 2 (as for the industrial FeMo catalysts used for methanol oxidation to formaldehyde) and heated under vigorous stirring to a temperature between 50 and 60 °C. The pH of the ammonium molybdate tetrahydrate solution was adjusted at 1 by adding concentrated HCl. Afterwards, the $FeCl_3{\cdot}H_2O$ solution was slowly added dropwise to the AHM solution and a yellow precipitate was obtained. The stirring was kept for 1 h and followed by several hours of decantation. Then, a chloride removal step was performed by washing the obtained precipitate with distilled water until the Cl^- content became lower than 2000 ppm. Later, the precipitate was filtrated and subsequently dried in an oven at 120 °C for 4 h. The obtained solid was crushed in a mortar and mixed with 1 wt.% of stearic acid before calcination under air flow (0.3 mL/min) at 450 °C. The way we will call the samples is the following: FeMoLa(Ce)*X*, where *X* is the Mo/Fe ratio and La or Ce as doping element.

In the case of doped FeMo catalysts, nitrate solutions of lanthanum and cerium [1 mol%] were prepared and added to the iron chloride solution at the very beginning of preparation. During the synthesis of these materials, the Mo/Fe ratios were varied (*i.e.*, from 1.5 to 2.5) as well as the calcination temperature (*i.e.*, 350, 400 and 450 °C).

2.3. Characterization

The freshly prepared dried samples (non-calcined) were analyzed by thermogravimetric analysis (TGA) and differential scanning calorimetric analysis (DSC) using a TA Instruments SDT-Q600 apparatus with alumina as a reference. The measurement was performed under air flow (100 mL/min) while increasing the temperature to 600 °C at a rate of 5°/min up).

High-temperature X-ray diffraction (XRD) was performed using a Brüker D8 apparatus (Brüker AXS, Cu-$K_{\alpha 1}$ λ = 1.5406 Å) to follow the temperature of phases crystallization. The analysis was performed under air flow from 50 °C to 500 °C with a heating rate of 10°/min. The diffractograms were recorded each 25 °C for 2θ values in the 10° to 60° range, using a 0.02° step and a 0.5 s integration time. The results

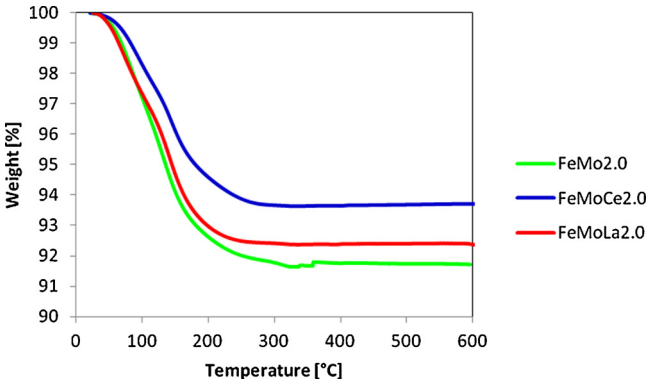

Fig. 1. TG for: FeMo2.0, FeMoLa2.0, FeMoCe2.0. The analysis was performed in the 20–600 °C temperature range with heating rate of 10 °C/min under air flow.

interpretation was made based on the database from the Joint Committee on Powder Diffraction Standards (JCPDS) using the EVA X-ray diffraction analyses software.

X-ray photoelectron spectroscopy (XPS) was performed using a Kratos Axis spectrometer apparatus with an alumina Kα radiation (1486.6 eV) under vacuum. All the results were treated using the CasaXPS software, and the surface compositions were determined from the various observed peaks (*e.g.*, Mo 3d, Fe 2p…) recorded at a 40 eV pass energy. The reference was taken for the C 1 s level binding energy for C-(C, H) bonds fixed at 285 eV.

Low energy ion scattering (LEIS) experiments were performed in a Qtac100 instrument (ION-TOF GmbH) at a pressure of 10^{-8} mbar. This instrument is fitted with a double toroidal energy analyzer (DTA), which collects the scattered ions at a scattering angle of 145° from all azimuth angles. The samples were analyzed using a 3 keV He^+ primary ion beam directed perpendicularly to the target surface. The area of analysis is 1 mm x 1 mm and the experiments were performed with a total dose per spectrum of $1{,}9 \times 10^{14}$ ions/cm^2. Quantification and simulation of the peaks were carried out using the SurfaceLab software. As LEIS is highly sensitive to the outermost surface, before analysis, the pressed samples were cleaned from carbon contamination by using an atomic oxygen plasma ($1–2 \times 10^{-5}$ mbar, 10 min).

The specific surface area was measured using the single-point BET method (Brunauer, Emmett, Teller) based on nitrogen adsorption and desorption using Micrometrics Flowsorb II Surface Area Analyzer. The analysis was performed on 200 mg of calcined catalyst placed in a glass chamber and outgassed at 150 °C during 20 min in order to remove the surface impurities. Afterwards, the glass chamber was dived in liquid nitrogen in order to perform the adsorption/desorption procedure followed by a TCD signal.

X-ray fluorescence (XRF) was performed for calcined samples using a S2Ranger Bruker apparatus placed in a tube through Mylar Sheet 6 microns under helium flow.The presence of basic sites on the catalysts' surface was examined with CO_2-temperature programmed desorption (CO_2-TPD). The measurement was performed on calcined samples with Micrometrics Autochem 2920 apparatus coupled with a MS Pfeiffer. First, the catalysts were pretreated under a He flow (50 mL/min) at 200 °C (temperature reached at a rate of 10 °C/min) during 1 h. Then, CO_2 adsorption was performed at room temperature during 30 min using a carbon dioxide flow (5% CO_2, 95% He). Finally, desorption was performed until 700 °C (this temperature being reached at a rate of 10 °C/min) during 30 min in helium (30 mL/min).

The presence of acid sites on the catalysts was measured by pyridine adsorption followed by FT-IR spectroscopy. The adsorption line was coupled with a Nicolet Protege 460 infrared spectrometer equipped with a MCT detector allowing the quantification of the acidic sites. Before analysis, weighted catalysts were ground in an agate mortar and pressed to get self-supporting wafers. Then, they were placed in the

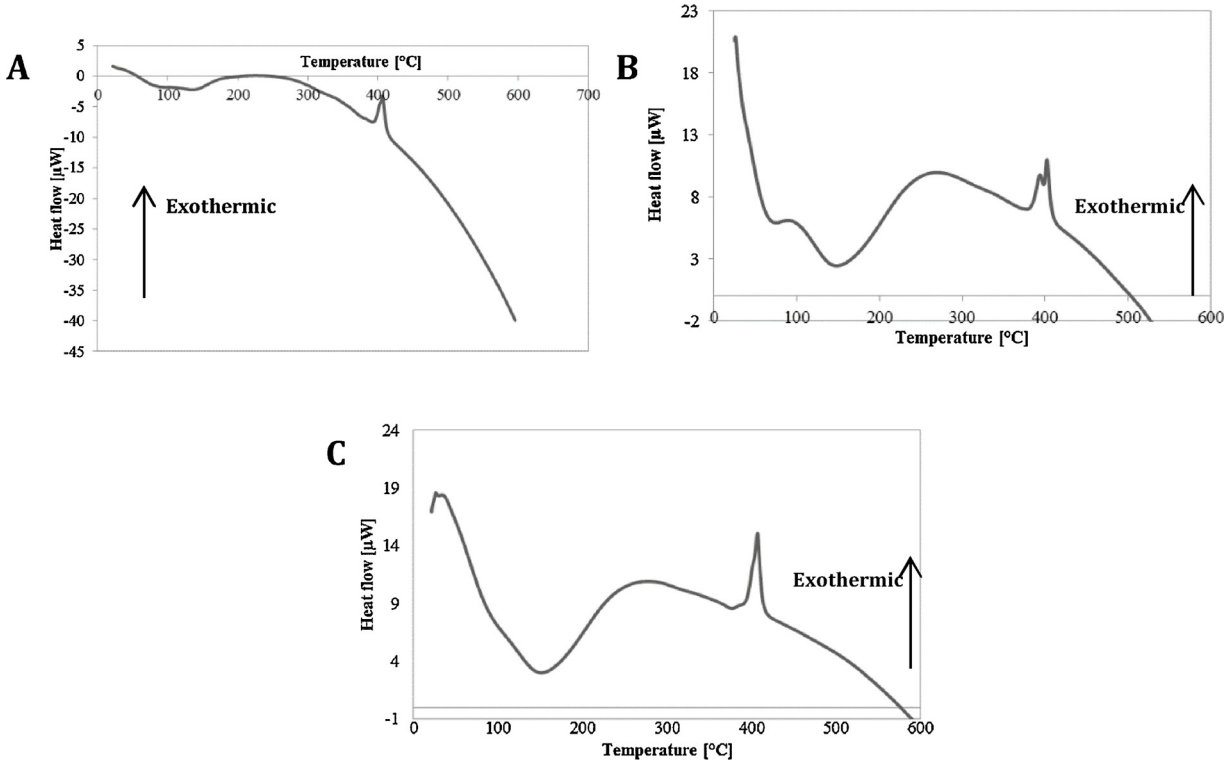

Fig. 2. DSC profile for FeMo2.0. The analysis was performed in the 20–600 °C temperature range with a heating rate of 10 °C/min under air flow.

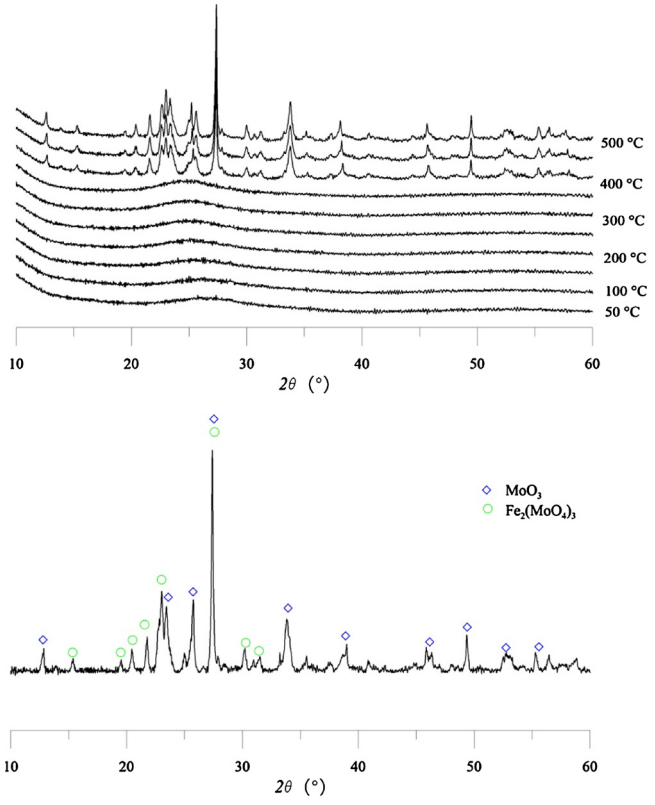

Fig. 3. Top)-HT diffractograms for FeMoCe2.0; Bottom) XRD pattern at room temperature with phases matching for FeMoCe2.0 calcined at 500 °C.

experimental setup under vacuum for 30 min, before being activated at 450 °C under dynamic vacuum for 2 h. After cooling to room temperature, pyridine was introduced at the equilibrium pressure of 1 Torr. Afterwards, the non-adsorbed molecules were evacuated under vacuum at ambient temperature during 10 min. After several repetitions, desorption was performed by maintaining a dynamic vacuum and heating. IR spectra were taken at several temperatures: 50, 150, 250 and 350 °C. In order to quantify the Lewis and Brønsted acid sites, FTIR spectrum of the initial activated surface was subtracted from that of the Pyridine adsorbed one. The following bands and adsorption coefficients were used: pyridinium (PyH^+ = Bronsted site) band located at 1525 cm^{-1}, ε_B = 1.23 cm/µmol and pyridine (PyL = lewis site) band located at 1454 cm^{-1}, ε_L = 1.73 cm/µmol [23].

The acid sites analysis was performed by adsorption microcalorimetry of NH_3. The experiments were performed at 150 °C in a heat flow calorimeter (C80 from Setaram) linked to a conventional volumetric apparatus equipped with a Barocel capacitance manometer for pressure measurements. The samples were pretreated overnight in a quartz cell under vacuum at 300 °C. The differential heats of adsorption were measured as a function of coverage by repeatedly sending small doses of gas probe (NH_3) onto the sample until an equilibrium pressure of around 67 Pa was reached. The sample was then outgassed for 40 min at the same temperature, and a second adsorption run was performed at 150 °C on each sample, until an equilibrium pressure of about 27 Pa was reached. The difference between the amounts adsorbed in the first and second adsorptions at 27 Pa represents the irreversibly adsorbed amount (V_{irr}) of ammonia, which provides an estimation of the number of strong acidic sites.

2.4. Catalytic performance measurement

The catalytic tests were performed in a glass fixed bed reactor with an internal diameter of 10 mm. For each run, 200 mg of catalyst (particle diameter 125 µm) mixed with 200 mg of SiC (particle diameter 125 µm) were used. The overall methanol and ethanol concentration in the reactor gas feed was chosen as 13.2 Vol. % with a molar ratio between the alcohols of 1. The reactor gas feed also comprised oxygen (12 Vol. %) and helium (74.8 Vol %). Before introduction in the reactor, the alcohols mixture was passed through an evaporator heated at 120 °C. The GHSV (calculated as Gas Flow Rate in standard conditions (25 °C,

Table 1
XPS results for the synthetized doped-FeMo catalysts and the reference FeMo2.0 catalyst.

Catalyst	Position		FWHM		Atom concentration [%]			Mo/Feratio
	$Mo3d_{5/2}$	$Fe2p_{3/2}$	$Mo3d_{5/2}$	$Fe2p_{3/2}$	Mo	Fe	C	
FeMo2.0	232.8	711.9	1.10	2.83	16.8	6.4	26.1	2.6
FeMoCe1.5	232.9	711.9	1.16	2.74	17.5	4.8	25.0	3.6
FeMoLa1.5	233.0	711.9	1.20	2.85	10.6	3.8	49.5	2.8
FeMoCe2.0	232.9	711.9	1.14	2.66	11.9	2.6	48.4	4.6
FeMoLa2.0	232.8	711.8	1.09	2.85	16.7	4.5	29.5	3.7
FeMoCe2.5	232.9	711.8	1.18	2.61	15.1	4.0	33.8	3.8
FeMoLa2.5	232.9	712.3	1.24	3.12	12.6	3.2	43.9	3.9

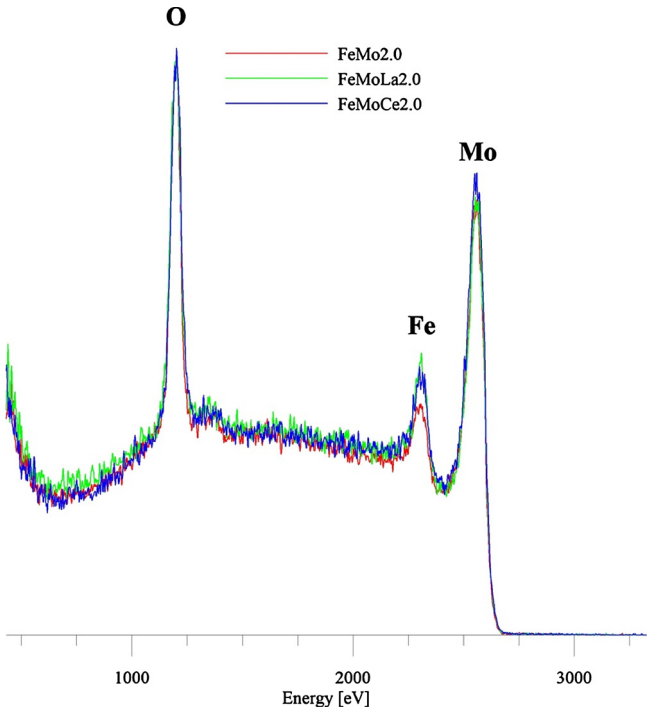

Fig. 4. LEIS spectra of FeMoLa2.0, FeMoCe2.0 and FeMo2.0. (The LEIS spectra are normalised regarding the O peak).

Table 2
SSA and Mo/Fe ratios (obtained from LEIS experiments) of FeMo2.0, FeMoCe2.0 and FeMoLa2.0.

Sample	SSA [m^2/g]	LEIS Mo/Fe ratio
FeMo2.0	5 +/- 1	6.7 (± 0.9)
FeMoCe2.0	8 +/- 1	5.5 (± 0.2)
FeMoLa2.0	12 +/- 1	4.5 (± 0.2)

Table 3
XRF results for FeMo and modified FeMo catalysts calcined in 450 °C.

Catalyst	Molar concentration [%]				Mo/Fe Ratio	Mo/Fe XPS Ratio
	Mo	Fe	La	Ce		
FeMo2.0	20.1	7.8	–	–	2.6	2.6
FeMoCe1.5	18.9	9.7	–	Trace	1.9	3.6
FeMoLa1.5	19.4	8.9	Trace	–	2.2	2.8
FeMoCe2.0	20.4	7.3	–	0.001	2.8	4.6
FeMoLa2.0	20.1	7.9	Trace	–	2.5	3.7
FeMoCe2.5	20.4	7.3	–	0.001	2.8	3.8
FeMoLa2.5	20.1	7.9	Trace	–	2.6	3.9

atmospheric pressure)/Catalyst Volume (measured based on reactor diameter and catalytic bed length)) was fixed at 3900 h^{-1} and the temperature of reaction was fixed at 320 °C. The exit of reactor was connected with a GC–MS apparatus for online analysis each 10 min (GC–MS, Agilent Technologies, 7890 A GC System, 5975C VL MSD with Triple Axis Detector equipped with a ZB-Bioethanol capillary column, Zebron, length 30 m, I.D. 0.25 mm, film thickness 1.0 µm). Conversion (X_{MetOH}, X_{EtOH}) and acrolein, formaldehyde, acetaldehyde and CO_2 yields (Y_{AC}, Y_{Formol}, Y_{MetCHO}, Y_{CO2}) were calculated using the following equations (Eqs. (3)–(8)):s

$$X_{MetOH} = \frac{n_{MetOH,in} - n_{MetOH,out}}{n_{MetOH,in}} \cdot 100\% \quad (3)$$

$$X_{EtOH} = \frac{n_{EtOH,in} - n_{EtOH,out}}{n_{EtOH,in}} \cdot 100\% \quad (4)$$

$$Y_{AC} = \frac{3 \cdot n_{AC}}{n_{MetOH,in} + 2 \cdot n_{EtOH,in}} \cdot 100\% \quad (5)$$

$$Y_{Formol} = \frac{n_{Formaldehyde}}{n_{MetOH,in} + 2 \cdot n_{EtOH,in}} \cdot 100\% \quad (6)$$

$$Y_{MetCHO} = \frac{2 \cdot n_{MetCHO}}{n_{MetOH,in} + 2 \cdot n_{EtOH,in}} \cdot 100\% \quad (7)$$

$$Y_{CO2} = \frac{n_{CO2}}{n_{MetOH,in} + 2 \cdot n_{EtOH,in}} \cdot 100\% \quad (8)$$

3. Results and discussion

The calcination temperatures and the crystallization process were observed using TGA-DSC analysis. A similar behavior was observed over all the synthesized materials. Thus, we present here, as examples, the results for the catalysts with a Mo/Fe ratio of 2.0 (Fig. 1) shows the weight evolution *vs.* temperature during the analysis. It can be observed that the weight loss starts at 100 °C due to water production/desorption from precursors decomposition. Decomposition continues until 300 °C and the catalyst weight loss reaches 6 to 9 wt % (Fig. 2).

Analyzing DSC evolutions, first an endothermic peak is observed at the temperature between 100 and 200 °C, which corresponds to the aforementioned precursors' decomposition. Then, an exothermic phenomenon is observed at the temperature close to 400 °C. It is assigned to crystallization of phase(s) present on catalyst surface which are identified thanks to XRD-HT measurement. Obtained results are aligned as well with studies on iron molybdate catalyst published in the literature [13].

All the synthetized samples were analyzed before calcination using an HT-XRD method. As we again observed a similar behavior over all the samples, we present the results obtained for FeMoCe2.0 as an example (Fig. 3). We can observe that the crystallization process starts at a temperature between 350 °C and 400 °C. At this latter temperature, two crystalline phases were identified: $Fe_2(MoO_4)_3$ (#PDF 00-031-0642) and MoO_3 (#PDF 01-089-5108), which are characteristic for

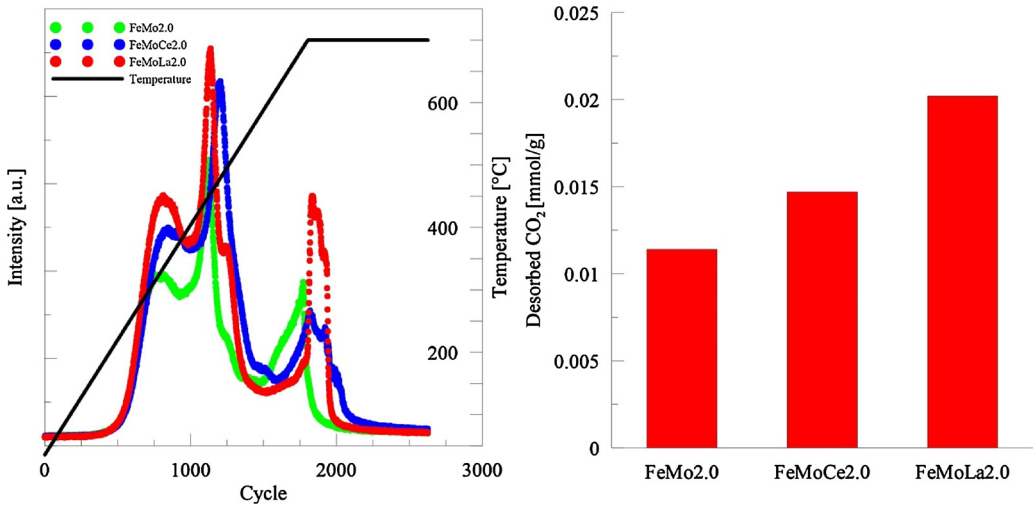

Fig. 5. CO_2-TPD results for FeMo2.0, FeMoCe2.0 and FeMoLa2.0 calcined at 450 °C.

iron-molybdate catalysts and which are the active phases of this material. The first step of the studied reaction consists on the oxidation of alcohols into aldehydes. The industrial catalysts used for these reactions are the crystalline form of FeMo catalysts. So we have chosen based on this observation to calcine the precursors at 450 °C to have the crystalline phases.

The surface of the catalysts was characterized using XPS. It was observed that iron is present only at the + III oxidation state (i.e., BE = 711.8 to 712.3 eV) while molybdenum is at the + VI oxidation state (i.e, BE = 232.9 to 233 eV) [24,25,26,27]. These oxidation numbers are perfectly in agreement with those of the phases detected by XRD. The analysis results are presented in Table 1. Like for the non-doped FeMo samples, the surface Mo/Fe ratio obviously deviated from that of the theoretical composition. The addition of basic elements seems to increase this phenomenon (i.e., Mo/Fe ratio for FeMo2.0 equals 2.6 while for FeMoCe2.0 we have observed 4.6 and for FeMoLa2.0–3.7).

La and Ce were not detected at the surface of the catalysts, which can be due to *i)*their low quantities introduced during the preparation, *ii)*the way they have been introduced in the solids (i.e., coprecipitation method and not impregnation) so that they can be supposedly "trapped" in the bulk of the solids, or *iii)*the fact that La 3d and Ce 3d signals can be hidden by the Auger signal of Iron (main peak for Ce3d @ ~882 eV (range 875–920 eV), main peak for La 3d @ ~835 eV (range 825–870 eV) and Fe Auger Fe LMM peak (830–920 eV)). In order to clarify this point, we performed LEIS analysis for FeMo2.0, FeMoCe2.0 and FeMoLa2.0. This technique enables probing the first atomic layer of the samples (Fig. 4).

Only three peaks assigned to O, Fe and Mo were detected. The absence of Ce and La signals on these spectra is a direct evidence that such species were actually not present at the upmost surface of the materials. Further, this suggests that any modification of the basic character of the catalyst would be an indirect phenomenon. Probably, lanthanum and cerium could have not been measured because the LEIS detection limit is in the 10–500 ppm of a monolayer range for higher masses elements (initially 10,000 ppm of Ce and La were introduced). Moreover, these two LEIS spectra (i.e., FeMoCe2.0 and FeMoLa2.0) are similar to that of the FeMo reference catalyst, but with different relative intensities. The LEIS surface Mo/Fe ratio was calculated (Table 2), which would show that the introduction of basic elements caused a changes in the Mo/Fe ratio to the extreme surface (i.e., first atomic layer) compared to the non-doped FeMo catalyst (i.e., Mo/Fe ratio decreases by up to 2.2 points).

In order to confirm the actual incorporation of the basic elements, which were not detected neither by XPS nor by LEIS, X-ray fluorescence experiments were performed. The catalysts calcined at 450 °C were analysed (Table 3). La and Ce were detected in very low concentrations (limit of detection of the apparatus) and their accurate quantification was thus not possible. These additives are then mostly located in the catalyst bulk. The Mo/Fe ratios in the catalysts bulk was determined as well by this method (Table 3). The obtained values are lower than those determined by XPS, but follow the trend of the theoretical values. These results suggest a migration of molybdenum species at the surface of the solids.

The specific surface areas of the catalysts calcined at 450 °C are presented in Table 2. The observed values are low and no clear trend could be observed.

The La and Ce addition was expected to bring more basic sites to the FeMo catalyst, which would theoretically improve the second process stage (i.e., formaldehyde and acetaldehyde dehydrogenation and condensation). These elements were not present at the surface of the solids (XPS, LEIS), however their presence induced a change in the Mo/Fe ratios. Thus, we decided to check the potential indirect influence of their introduction on the acid-base properties of the synthesized materials. CO_2-TPD analysis was performed for the FeMo2.0, FeMoCe2.0 and FeMoLa2.0 samples calcined at 450 °C (Fig. 5).

First of all, the CO_2 desorbed quantities were very low due to the very low SSAs (at max 10 m^2/g). The CO_2 desorption occurred at different temperatures, according to the different strengths of the basic sites. All the samples exhibited 3 peaks at approximately 300, 450 and 700 °C, characteristics of weak, medium basic and strong basic sites, respectively. The total desorbed carbon dioxide quantities were calculated and are presented in Fig. 5. The introduction of La and Ce in the FeMo-based catalysts actually induced an increase in the total number of basic sites, which is an indirect phenomenon, as these elements are not present at the surface (i.e., absence of signal in XPS and LEIS). The two doped materials present an increase in the number of each site compared to the non-doped one. The La-doped material presents a dramatic increase in the number of strong basic sites compared to the two other catalysts.

As previously shown [13], the FeMo-based catalysts also present acid sites. In order to deeply characterize such sites, we performed pyridine adsorption followed by IR. This probe molecule allows identifying both type of sites [i.e., Brønsted (B) and/or Lewis (L)] as well as quantifying their respective quantities (Fig. 7). As observed for the basic sites, the concentration in acid sites is quite low due to the low SSA of the materials. The FTIR spectra were recorded after pyridine adsorption and thermal treatment at different temperatures. After heating at 350 °C (catalyst activation temperature), no signal was observed, indicating that the catalysts do not have very strong acid sites.

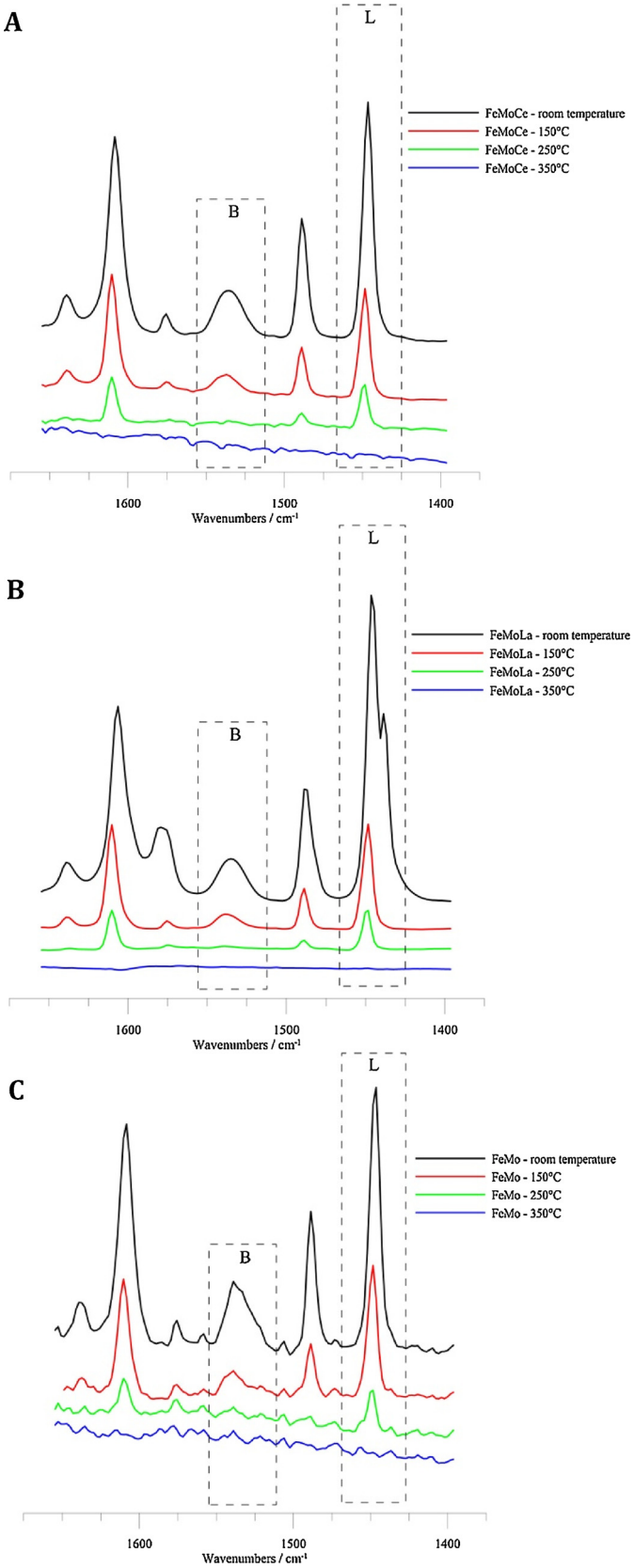

Fig. 6. Pyridine adsorption/desorption at different temperatures (*i.e.*, 150, 250 and 350 °C). Normalized spectra of: A: FeMoCe2.0, B: FeMoLa2.0, C: FeMo2.0 calcined at 450 °C (B- Brønsted sites, L- Lewis sites) after activation.

However, the presence of Lewis acid sites was observed. Comparing to Brønsted ones the number of these sites is larger (Fig. 6) and the doping seems to affect more the Lewis acid sites than the Brønsted ones. The sample presenting the highest acid site number is also that presenting the highest basic sites numbers: FeMoLa2.0 (12 µmol/g). Comparing with the results obtained by CO_2-TPD shown above (Fig. 5), we can conclude that the addition of La generates not only basic sites but also acid sites [10].

Fig. 7. Quantity of desorbed pyridine on FeMo2.0 and FeMoCe2.0 at 50 °C. A: Lewis sites; B: Brønsted sites.

The acidity of the samples was additionally characterized by adsorption microcalorimetry of NH_3. This technique allows to determine the amount, strength and strength distribution of the acidic sites on the surface of the materials. Ammonia was used as a basic molecule, which is able to quantify both Lewis and Brønsted acidic sites [28,29]. Fig. 8 represents the curves of differential heats (Q_{diff}) of NH_3 adsorption *vs.* the amount of the probe molecule adsorbed as well as the total and irreversibly adsorbed amount of ammonia at 27 Pa for each sample. FeMoLa2.0 exhibited the highest acidity (i.e., the highest number of sites) due to its slightly higher specific surface area (SSA) compared to FeMo and FeMoCe2.0 samples, while the amount of adsorbed ammonia is relatively low for all three samples due to their relatively low SSA. However, the presence of strong acidic sites, characterized by $Q_{diff} > 100$ kJ/mol, [28,24] was observed over all the samples and the amount of these sites decreased in the order FeMoLa2.0 > FeMo > FeMoCe2.0 (Fig. 8a). In particular, the presence of a few very strong acidic sites ($Q_{diff} > 150$ kJ/mol) was observed at the surface of the FeMoLa2.0 catalyst, which was not detected by pyridine adsorption experiments due to their differences in terms of kinetic diameters. It can be observed (Fig. 8b) that the total and irreversibly adsorbed amount of ammonia is the highest for FeMoLa2.0 catalyst. The total amount of acidic sites of the samples can be classified in the following order: FeMoLa2.0 > FeMoCe2.0 ≥ FeMo, which is in agreement with the results obtained by pyridine adsorption (Fig. 7).

The catalytic activity of the modified FeMo catalysts was evaluated using a mixture of methanol and ethanol and oxygen in inert carrier (He) in optimal conditions found previously [11] (i.e., GHSV = 3900 h^{-1}, O_2 = 12%, Temperature = 320 °C, MeOH/EtOH = 1 mol/mol). The following products were detected: acrolein, acetaldehyde, formaldehyde, carbon dioxide, dimethyl ether (traces) and methoxyethane (traces), similarly to the observation over conventional FeMo. In order to check the influence of the additives on the acrolein yield, the FeMo2.0 sample calcined at 450 °C (i.e., 36.5% of acrolein yield) was chosen as the reference catalyst.

Fig. 9 presents the evolution of the products' yields in time for FeMo2.0 samples before and after the modification with basic elements calcined at 450 °C. It can be remarked that the selectivity to acrolein slightly increased over doped catalysts (i.e., +2.5% in terms of acrolein yield for FeMoCe2.0 and +1.5% for FeMoLa2.0). In terms of by-products, an increase in formaldehyde yield and a decrease in acetaldehyde yield were observed.

Afterwards, the different synthesized catalysts with various Mo/Fe ratios, different calcination temperatures and with doping elements were tested (Table 4). In all cases, the alcohols conversions reached 100%. The highest yield of acrolein was observed for FeMoCe2.0 (400 °C): 42%, which is a + 5 points improvement compared to pure FeMo. Similarly, 4 points of improvement were observed for FeMoLa2.5 (400 °C), which confirms the positive influence of lanthanum addition.

At this stage, it is not straightforward to claim that the increase of acrolein yield is due to the increase in basic and acid site numbers due to the fact that the second part of the reaction (i.e., aldol condensation reaction) needs both types of sites [10]. It is however factual that the introduction of basic elements led to an increase in the number of acid/base pairs then to an improvement of the target molecule yields.

Concerning the influence of the calcination temperature, similarly to conventional FeMo, the lowest acrolein yield was in most cases (with

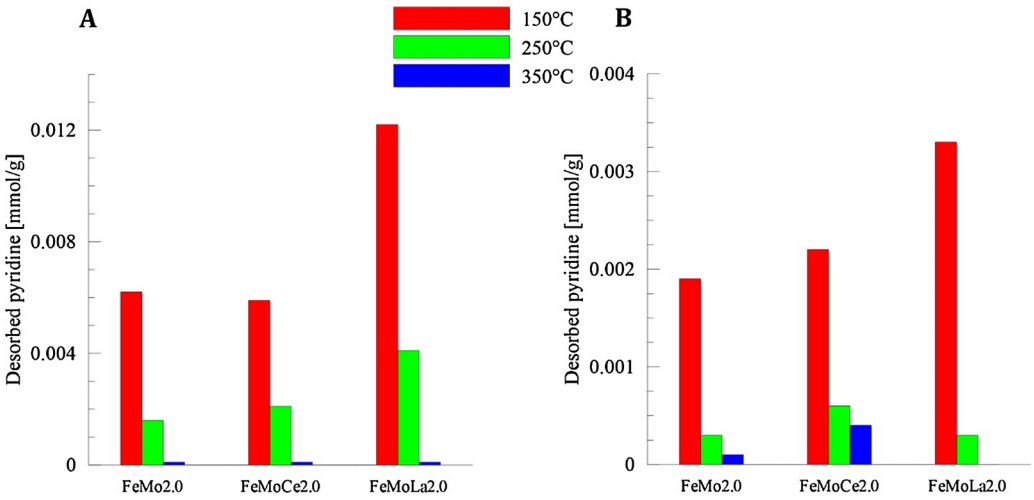

Fig. 7. Quantity of desorbed pyridine on FeMo2.0 and FeMoCe2.0 at 50 °C. A: Lewis sites; B: Brønsted sites.

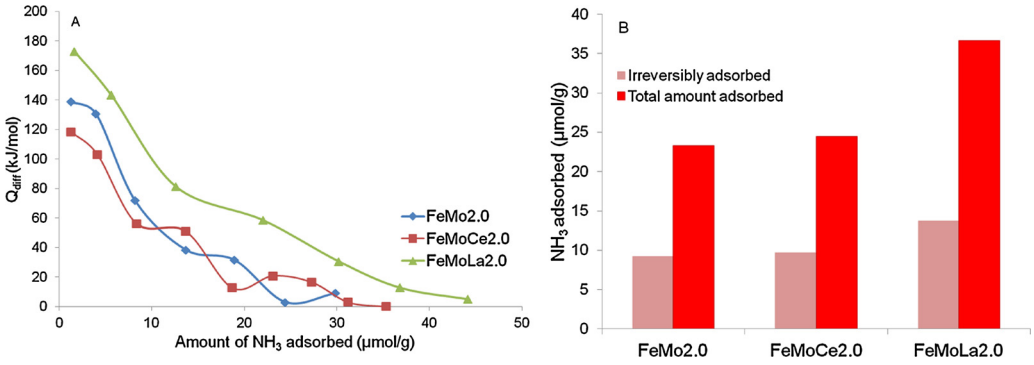

Fig. 8. Differential heats of NH_3 adsorption as a function of ammonia adsorbed (A) and comparison of total and irreversible amount of ammonia adsorbed (B) for FeMo2.0, FeMoCe2.0 and FeMoLa2.0.

the exception of FeMoLa1.5) observed for a calcination performed at 350 °C while the reactivity differences of samples calcined at 400 and 450 °C were not that significant (once again with the exception of FeMoLa1,5). The last studied point was the impact of the Mo/Fe ratio. Similarly to the pure FeMo series, the lowest acrolein quantity was observed over the catalyst with a Mo/Fe ratio equal 1.5 while the highest values are obtained for the ratio 2.0. This suggests that the minimal value favouring our target molecule production should not be lower than 2.0.

If we consider that the aldehydes could be recycled during the process and transform then to acrolein, provided that some conditions are defined to avoid their accumulation in the recycling loop, the FeMoLa1,5 and FeMoLa2,5 catalysts, present very interesting characteristics.

4. Conclusions

Our results show that the modification of iron-molybdate catalysts by doping with basic elements actually increase the number of both the acid and basic sites. This increase leads to a slight improvement in the desired acrolein quantity production through methanol and ethanol oxidative coupling. The catalytic activity of the obtained materials was measured and compared with that of FeMo2.0 calcined at 450 °C. The highest acrolein yield was obtained for FeMoCe2.0 calcined at 400 °C (*i.e.,* 42%) corresponding to an improvement of 5.5 points compared to the Ce-free sample. The catalyst modified with La brought also the expected improvement, with an acrolein yield of 40.5% (FeMoLa2.5 calcined at 400 °C). The bare FeMo catalyst and some doped catalysts are promising since they show less over-oxidation to CO_2, and higher yields to acetaldehyde, which is a valuable compound when considering an industrial process in which the co-products could be valorised or recycled. In order to understand the influence of the basic elements addition, several characterization methods were performed. First, thanks to XPS and LEIS analyses, it was found that La and Ce are not present at the top surface of the materials. However, LEIS analysis shows that their addition leads to a decrease in the surface Mo/Fe ratio contrary to XPS measurement. This can be explained by the relative analysis deepness of both analyses (one atomic layer for LEIS *vs.* a few atomic layers for XPS). It is noteworthy that XRF measurements proved that low quantity of La and Ce are actually present in the catalyst structure (bulk). The La and Ce addition influence on the catalyst basicity was checked using CO_2-TPD. The number of basic sites of the modified FeMo catalysts increased (medium and strong sites were formed), which suggests an indirect effect of La and Ce incorporation (as these elements are not present on the surface). Furthermore, based on acidity measurements (pyridine adsorption and microcalorimetry) it was observed that by La and Ce doping the acid sites number increases. This acid site number increase seems to lead to a better acid-base balance on the catalyst surface that is needed for formaldehyde and acetaldehyde condensation to form acrolein.

Acknowledgements

This project is supported by ADEME (The French Environment and Energy Management Agency) within the framework of the Investissements d'Avenir program ("Investment for the Future"). Chevreul Institute (FR 2638), Ministère de l'Enseignement Supérieur et de la Recherche, Région Nord – Pas de Calais and FEDER are

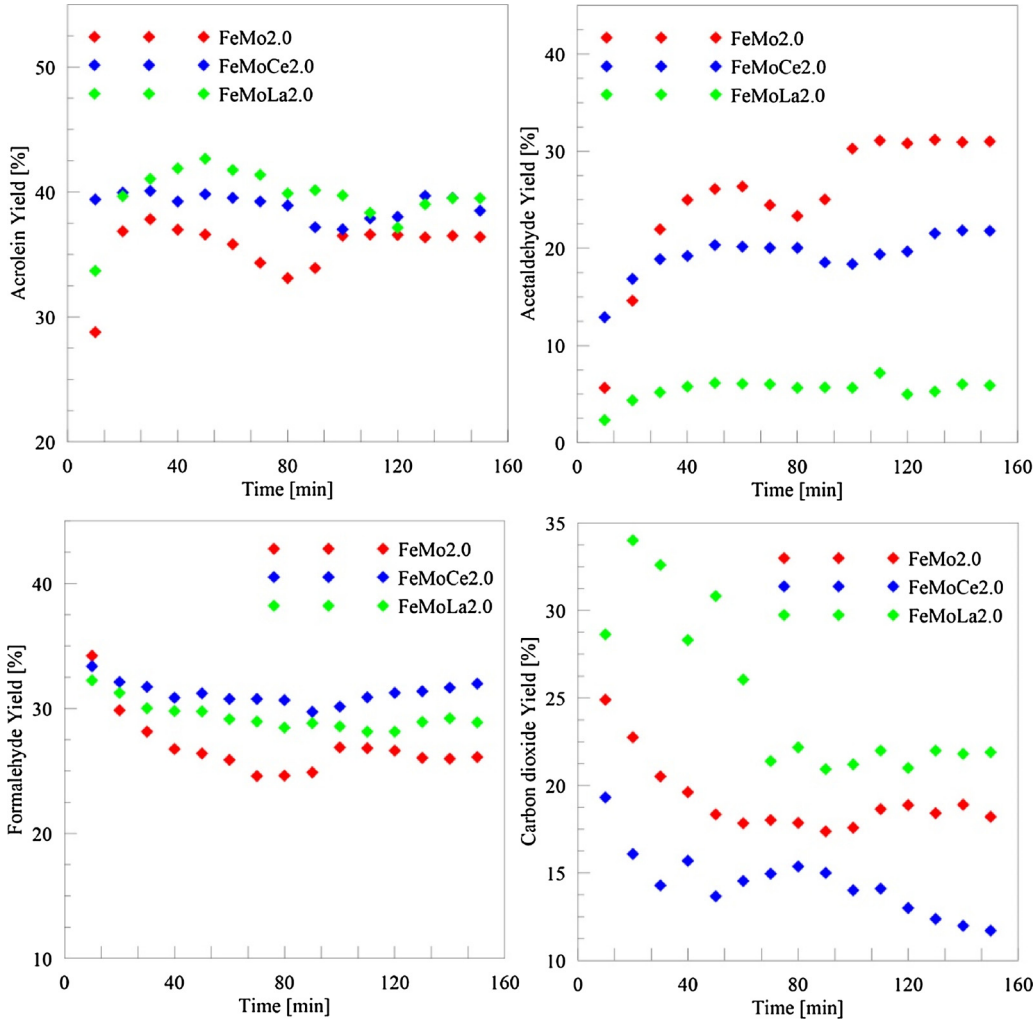

Fig. 9. Catalytic tests results for FeMo2.0, FeMoCe2.0 and FeMoLa2.0 (*i.e.*, GHSV = 3900 h^{-1}, O_2 = 12%, Temperature = 320 °C, MeOH/EtOH = 1 mol/mol).

Table 4
Catalytic tests' results over the synthetized FeMo catalysts (GHSV = 3900 h^{-1}, O_2 = 12%, Temperature = 320 °C, MetOH/EtOH = 1). Alcohols conversion are 100%.

Catalyst	Yield [%]			
	Acrolein	Acetaldehyde	Formaldehyde	CO_2
FeMo2.0(450 °C)	36.5	31	26	18.5
FeMoCe1.5(450 °C)	33.5	28	21	18
FeMoCe1.5(400 °C)	34	20.5	22	22
FeMoCe1.5(350 °C)	32	12	23	17
FeMoLa1.5(450 °C)	20	65	18	4
FeMoLa1.5(400 °C)	36.5	30.5	25	10
FeMoLa1.5(350 °C)	36.5	7	28	14
FeMoCe2.0(450 °C)	38	20	31	20
FeMoCe2.0(400 °C)	42	14	36	20
FeMoCe2.0(350 °C)	38	18	29	22
FeMoLa2.0(450 °C)	39	6	29	30
FeMoLa2.0(400 °C)	35	2	35	30
FeMoLa2.0(350 °C)	21	Trace	41	36
FeMoCe2.5(450 °C)	32	30	20	9
FeMoCe2.5(400 °C)	34	34.5	22	10
FeMoCe2.5(350 °C)	32	9	25	14
FeMoLa2.5(450 °C)	35.5	26.5	20	10
FeMoLa2.5(400 °C)	40.5	22	20	13.5
FeMoLa2.5(350 °C)	30	11	20	20

acknowledged for supporting and funding partially this work.

Gratitude to Olivier Gardoll, Laurence Burylo, Pardis Simon, Martine Trentesaux, Anne-Sophie Mamede and Maxence Vanderwalle for their precious help with catalysts characterization.

References

[1] T. Ohara, T. Sato, N. Shimizu, G. Prescher, H. Schwind, O. Weiberg, K. Marten, H. Greim, Acrylic Acid and Derivatives. Ullmann'S Encyclopedia of Industrial Chemistry, (2011).
[2] W. Bauer, Acrylic Acid and Derivatives. Kirk-Othmer Encyclopedia of Chemical Technology, (2003).
[3] D. Arntz, A. Fischer, M. Höpp, S. Jacobi, J. Sauer, T. Ohara, T. Sato, N. Shimizu, H. Schwind, Acrolein and Methacrolein. Ullmann's Encyclopedia of Industrial Chemistry, (2011).
[4] L. Liu, X.P. Ye, J.J. Bozell, ChemSusChem 5 (2012) 1162.
[5] B. Katryniok, S. Paul, M. Capron, F. Dumeignil, ChemSusChem 2 (2009) 719.
[6] B. Katryniok, S. Paul, M. Capron, C. Lancelot, V. Bellière-Baca, P. Rey, F. Dumeignil, Green Chem. 12 (2010) 1922.
[7] B. Katryniok, S. Paul, F. Dumeignil, Green Chem. 12 (2010) 1910–1913.
[8] Patent WO 2009127889 A1, assigned to Arkema France.
[9] PCT Patent Application WO2014068213, Assigned to Arkema France, (2013) Priority date Oct 17 Granted US patent US9365478.
[10] A. Lilić, T. Wei, S. Bennici, J.F. Devaux, J.L. Dubois, A. Auroux, ChemSusChem 10 (2017) 3459.
[11] A. Borowiec, J.F. Devaux, J.L. Dubois, L. Jouenne, M. Bigan, P. Simon, M. Trentesaux, J. Faye, M. Capron, F. Dumeignil, Green Chem. 19 (2017) 2666.
[12] A. Lilić, S. Bennici, J.F. Devaux, J.L. Dubois, A. Auroux, ChemSusChem 9 (2017) 1916.
[13] K. Thavornprasert, M. Capron, L. Jalowiecki-Duhamel, O. Gardoll, M. Trentesaux, A.S. Mamede, G. Fang, J. Faye, N. Touati, H. Vezin, J.L. Dubois, J.L. Couturier, F. Dumegnil, Appl. Catal. B 145 (2014) 126.

[14] F. Trifirò, I. Pasquon, la Chimica e l'Industria (Milan) 53 (1971) 577.
[15] H. Adkins, W.R. Peterson, J. Am. Chem. Soc. 53 (1931) 1513.
[16] A.P.V. Soares, M. Farinha Portela, A. Kiennemann, L. Hilaire, J.M.M. Millet, Appl. Catal., A 206 (2001) 221.
[17] J. Gornay, X. Secordel, M. Capron, G. Tesquet, P. Fongarland, J.L. Dubois, F. Dumeignil, Oil Gas Sci. Technol. 65 (2010) 751.
[18] J. Gornay, X. Secordel, G. Tesquet, B. de Menorval, P. Fongarland, M. Capron, L. Duhamel, E. Payen, J.L. Dubois, F. Dumeignil, Green Chem. 12 (2010) 1722.
[19] K. Thavornprasert, Thesis: Production of Acetals from Bio-Resourced Alcohols Over Bifunctional Catalysts, Lille 1 University, 2013.
[20] K. Thavornprasert, M. Capron, L. Jalowiecki-Duhamel, F. Dumeignil, Catal. Sci. Technol. 6 (2016) 958.
[21] N. Pernicone, F. Lazzeria, G. Liberti, G. Lanzavecchia, J. Catal. 14 (1969) 293.
[22] N. Pernicone, J. Less-Common. Metals 36 (1974) 289.
[23] M. Tamura, K. Shimizu, A. Satsuma, Appl. Catal. A 433 (2012) 135.
[24] Y.V. Plyuto, I.V. Babich, I.V. Plyuto, A.D. Van Langeveld, J.A. Moulijn, Appl. Surf. Sci. 119 (1997) 11.
[25] T. Yamashita, P. Hayes, Appl. Surf. Sci. 254 (2008) 2441.
[26] M.C. Biesinger, B.P. Payne, A.P. Grosvenor, L.W.M. Lau, A.R. Gerson, R. St, C. Smart, Appl. Surf. Sci. 257 (2011) 2717.
[27] A.P. Grosvenor, B.A. Kobe, M.C. Biesinger, N.S. McIntyre, Surf. Interface Anal. 36 (2004) 1564.
[28] A. Auroux (Ed.), Calorimetry and Thermal Methods in Catalysis, Springer Series in Materials Science, Springer-Verlag, Berlin Heidelberg, 2013, p. 154, , http://dx.doi.org/10.10097/978-3-642-11954-5_1.
[29] A. Auroux, Top. Catal. 4 (1997) 71.